Electronic Supplementary Information for

A Facile solution approach to photocatalytic active W, N co-doped TiO_2 nanobelt thin films

Lu-Lu Lai and Jin-Ming Wu*

State Key Laboratory of Silicon Materials and School of Materials Science and Engineering, Zhejiang University, Hangzhou, 310037, P. R. China

Experimental procedure

Synthesis of the W, N co-doped TiO_2 nanobelt films: Titanium plates with the size of 5 cm × 5 cm were etched at ambient conditions for 30 seconds in a mixture of 55 wt. % HF, 63 wt. % HNO_3 and distilled water, in a volume ratio of 1:3:6, followed by cleaning in distilled water with an ultrasonic bath. The cleaned Ti plate was placed on the bottom of a beaker (400 mL), which was filled with 50 mL 30 % H_2O_2 solution containing 2.4 mM melamine ($C_3H_6N_6$) and 40 mM H_2WO_4, and kept for 72 h in an oven maintained at 80 ^oC. The Ti plate was washed with distilled water, dried, and subjected to a final calcination in air at 450 ^oC for 1 h. For comparison purpose, TiO_2 thin films were also fabricated using the 30 % H_2O_2 solution only, that with the additive of either melamine or H_2WO_4 only.

Synthesis of TiO_2 nanobelt films *via* alkali-hydrothermal method: TiO_2 nanobelt films used for comparisons in photocatalytic activity were synthesized according to the literature with a little modification.[1] The cleaned Ti plate (2.5 × 2.5 cm^2 in size) was placed in a 50 mL Teflon-lined stainless steel autoclave filled with 35 mL 5 M NaOH aqueous solution. The sealed autoclave was put in an oven maintained at 180 °C for 24 h. After the reaction, the Ti plate was immersed in 0.1 M HCl aqueous solution for 40 min and the process was repeated for 3 times to fulfill the exchange between Na^+ with H^+. After the proton exchange treatment, the Ti plate was rinsed with water, dried at 80 ^oC, and subjected to the final calcination in air at 450 ^oC for 1 h.

Characterization

The morphologies of the samples were examined by a field-emission scanning electron microscopy (FESEM, Hitachi, S-4800) and a transmission electron microscopy (TEM, FEI, Tecnai G2 F20 S-TWIN). The X-ray diffraction (XRD) tests were performed using a XRD-6000 diffractometer (SHIMADZU) with a Cu Kα radiation, operated at 40 kV, 40 mA (λ=0.15406 nm). The Raman spectra were collected using an Almega dispersive Raman system (Nicolet) and a Nd:YAG in intracvity doubled laser operating at 532 nm with an incident power of 10 mW. The X-ray photoelectron spectra (XPS) characterization was carried out on an ESCA spectrometer (S-Probe ESCA SSX-100S, Fisons Instrument) and monochromatized Al Kα X-ray irradiation. The binding energy was calibrated by using the containment carbon (C 1s = 284.6 eV). The UV-Vis diffuse reflectance spectra were measured using a UV-Vis near-infrared spectrometer (UV-3600, Shimadzu). The ambient photoluminescence (PL) emission spectra were recorded by a fluorescence spectrophotometer (Hitachi, F-4500), with an exciting light 300 nm in wavelength.

Photocatalytic test

The photocatalytic activities of the calcinated films were evaluated by degradations of rhodamine B in water with an initial concentration of 0.005 mM. The UV+Vis illumination was provided directly by a 500 W Xe-lamp. For the visible light illumination, a filter was used to cut off light with wavelength less than 400 nm. The UV light was provided by an 18 W UV lamp. The light intensity was measured for the wavelength range of 320-400 nm with a peak wavelength of 365 nm for UV light, and 400-1000 nm for visible light (Model: UV-A and FZ-A, Beijing Normal University, China) and the data were listed in Table 1 in the main text. For each run, 25 mL rhodamine B solution in the presence of films with sizes of 2.5 × 2.5 cm^2 was firstly stirred in the dark for 60 min to reach an absorption-desorption equilibrium and then subjected to the specific light for different time period. The rhodamine B concentration was monitored with a UV-Vis spectrophotometer (UV-1800PC, Shanghai, Mapada) at the wavelength of 553 nm.

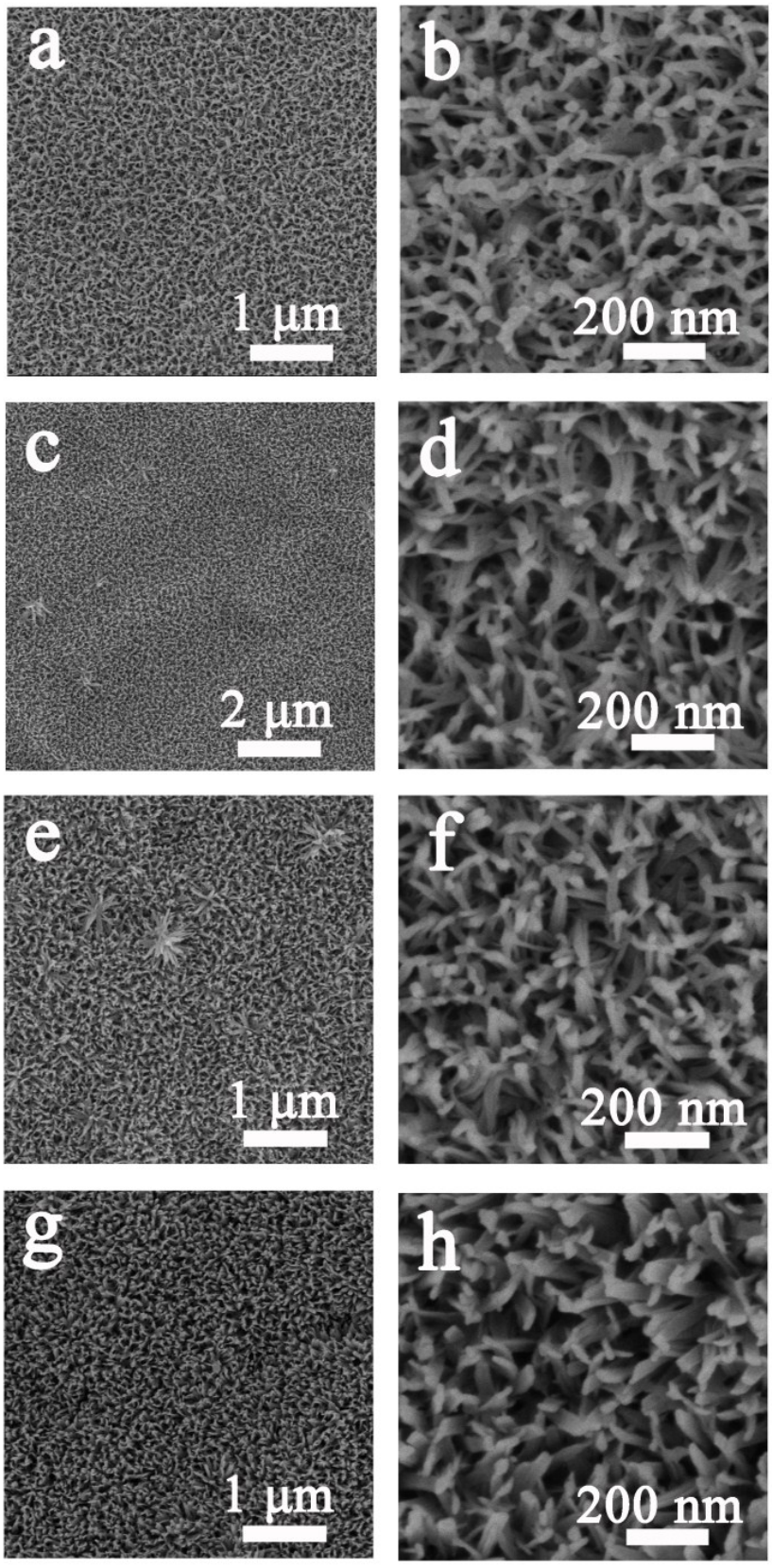

Figure S1. Morphology evolution of the Ti plate after oxidation in the H_2O_2 solution containing melamine and H_2WO_4 at 80 ^oC for various durations: (a, b) 6 h; (c, d) 12 h; (e, f) 24 h; (g, h) 48 h.

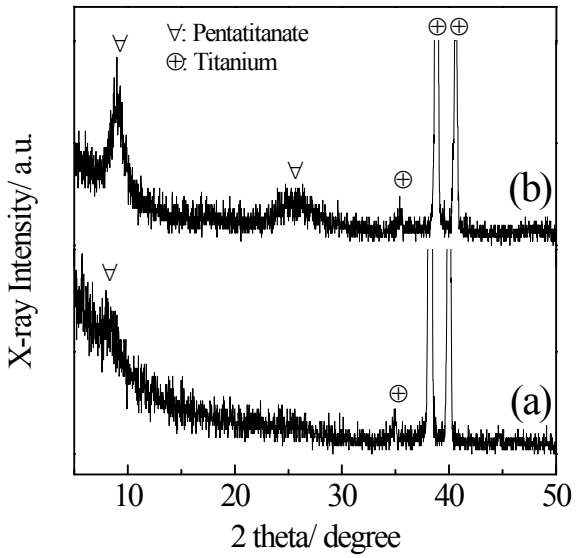

Figure S2. XRD patterns of the Ti plate after oxidation in the H_2O_2 solution containing melamine and H_2WO_4 at 80 °C for (a) 6 h and (b) 24 h.

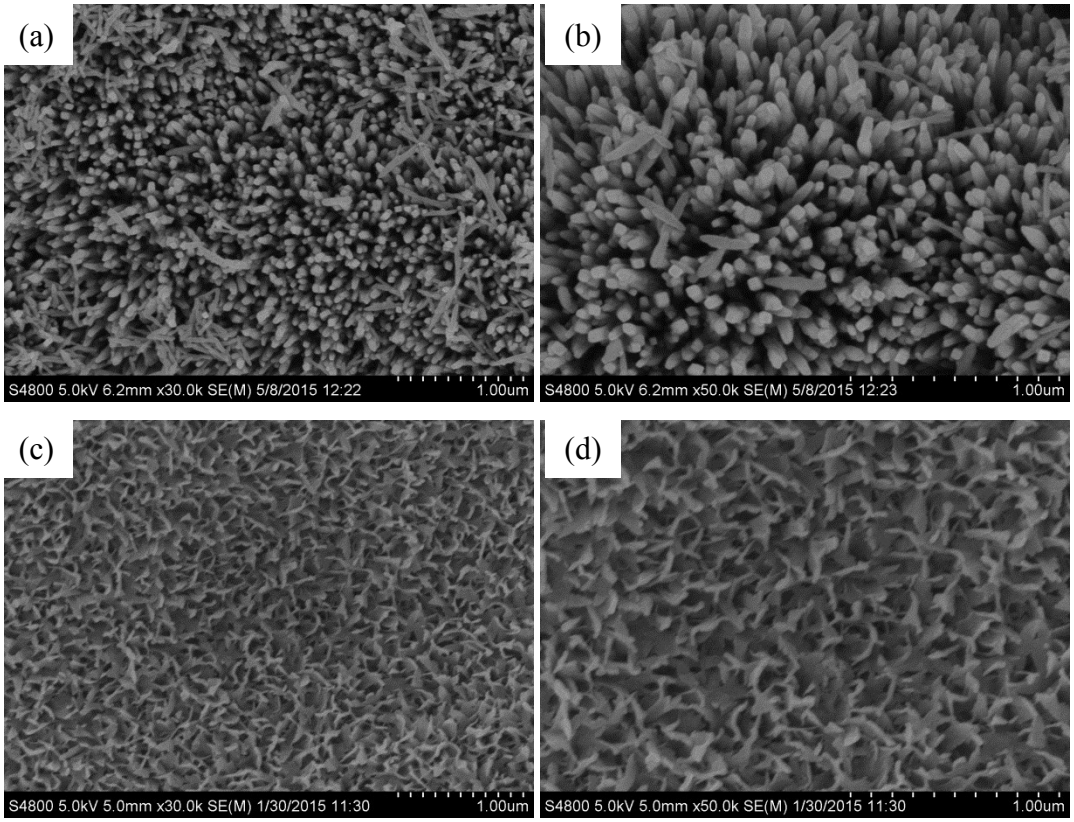

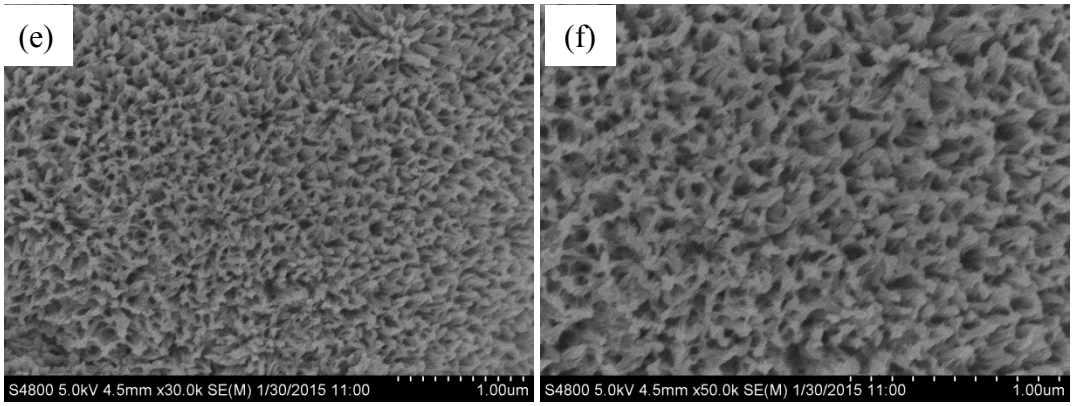

Figure S3. FESEM images of the Ti plate after oxidation at 80 °C for 72 h in the H_2O_2 solution (a, b), and that contained melamine (c, d), and H_2WO_4 (e, f). All the films were subjected to calcination in air at 450 °C for 1 h.

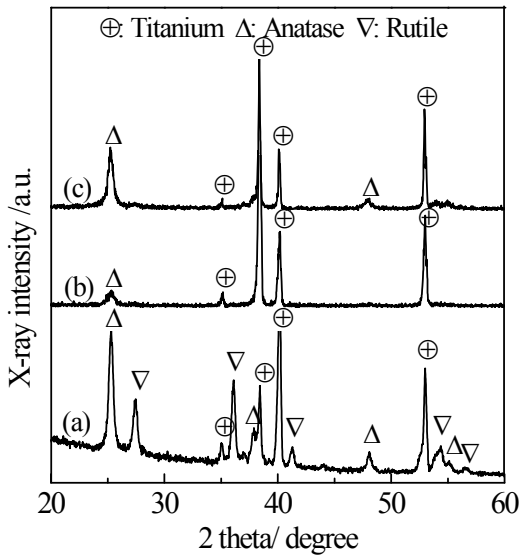

Figure S4. XRD patterns of the Ti plate after oxidation at 80 °C for 72 h in the H_2O_2 solution (a), and that contained melamine (b), and H_2WO_4 (c). All the films were subjected to calcination in air at 450 °C for 1 h.

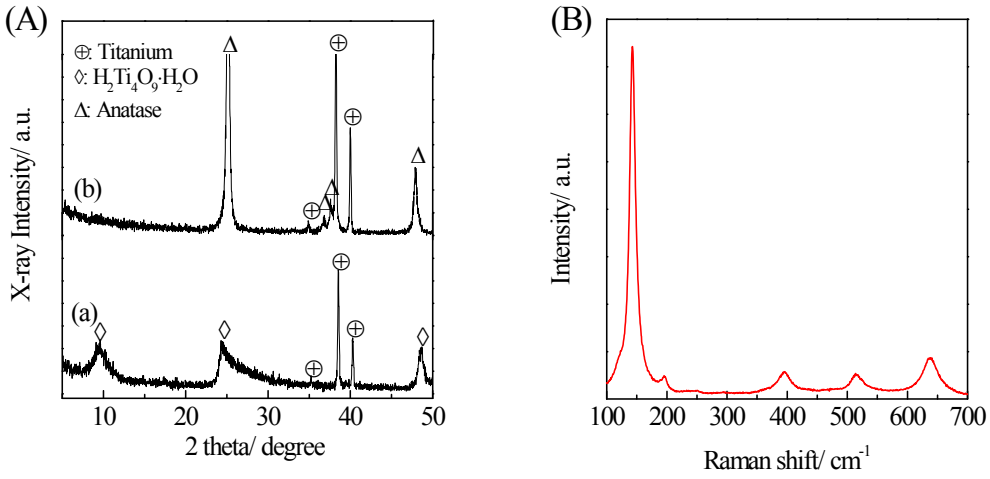

Figure S5. (A-b) XRD pattern and (B) Raman spectrum of the TiO_2 nanobelt film synthesized by the alkali-hydrothermal method. The XRD pattern of the as-synthesized titanate nanobelt was shown in (A-a).

The as-synthesized nanobelts can be indexed to $H_2Ti_4O_9·H_2O$ (JCPDS card No. 36-0655). After calcinating at 450 °C for 1 h, the $H_2Ti_4O_9·H_2O$ phase transformed thoroughly to anatase TiO_2. The Raman spectrum of the calcinated film further confirms that the alkali-hydrothermally synthesized nanobelts after calcination are anatase TiO_2.

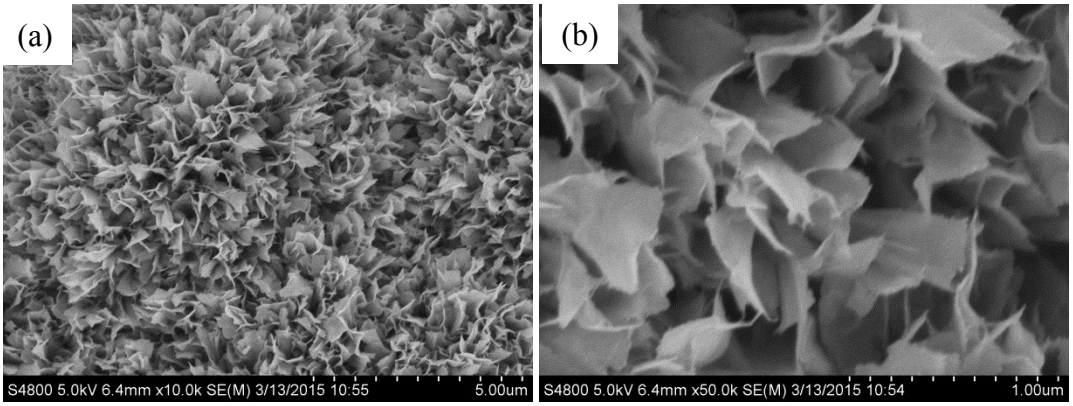

Figure S6. Low (a) and (b) high magnification FESEM images of the nanobelt film synthesized by the alkali-hydrothermal method.

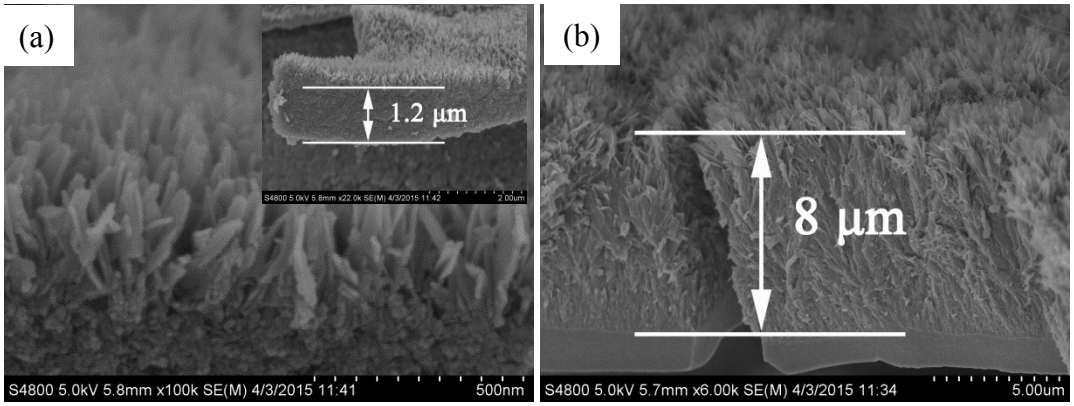

Figure S7. Cross-sectional FESEM images of the nanobelt films synthesized by (a) the present Ti-H_2O_2 reaction and (b) the alkali-hydrothermal method. The inset in (a) shows the immediate compact layer between the nanobelt film and the Ti substrate, which is 1.2 μm in thickness.

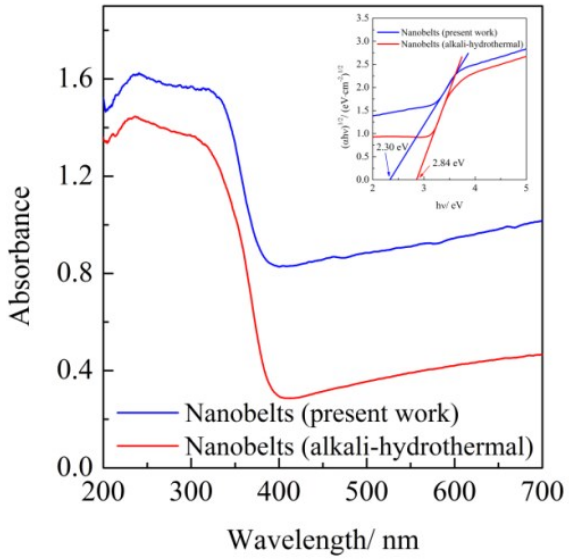

Figure S8. UV-Vis diffuse reflectance spectra of the TiO_2 nanobelt film synthesized by the alkali-hydrothermal method. The inset shows the spectrum in an $(\alpha h\nu)^{1/2} \sim h\nu$ coordinate to evaluate the corresponding band gap. Those for the W, N co-doped TiO_2 nanobelt thin film (demonstrated as Figure 4 in the main text) was also included for a direct comparison.

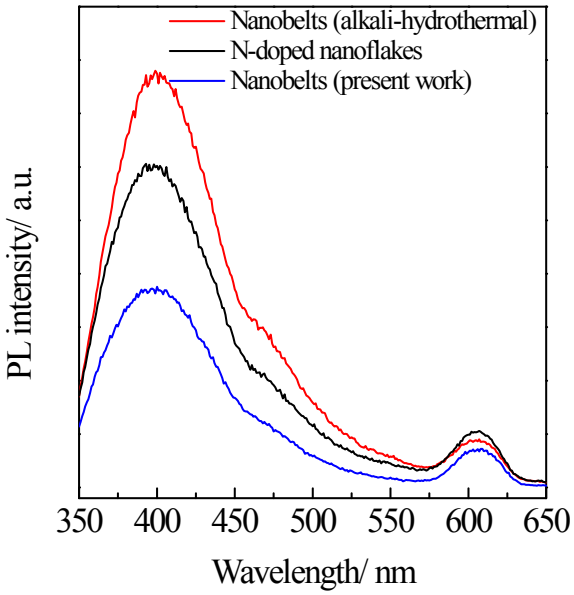

Figure S9. Room temperature photoluminescence emission spectra of the nanobelt films synthesized by the present Ti-H_2O_2 reaction (present work) and the alkali-hydrothermal method (alkali-hydrothermal). Also included is the single N-doped TiO_2 nanoflakes (see Fig. S3c, d for the film morphology).

The peak located at around 400 nm is related to the electron transition from the valence band to conduction band, that is, self-trapped excitons. The peak at 608 nm can be assigned to surface oxygen vacancies located at the surface of TiO_2. [2] The PL spectrum is related to the transfer behavior of the photoinduced electrons and holes, which hence reflects the separation and recombination of photoinduced charge carriers [3]. The intensity of the main peak located at ca. 400 nm decreased in the order of the alkali-hydrothermal derived dopants-free TiO_2 nanobelts, the single N-doped TiO_2 nanoflakes, and the W, N co-doped TiO_2 nanobelts. The W, N co-doping thus contributes to the reduced charge recombination and in turn the photocatalytic activity.

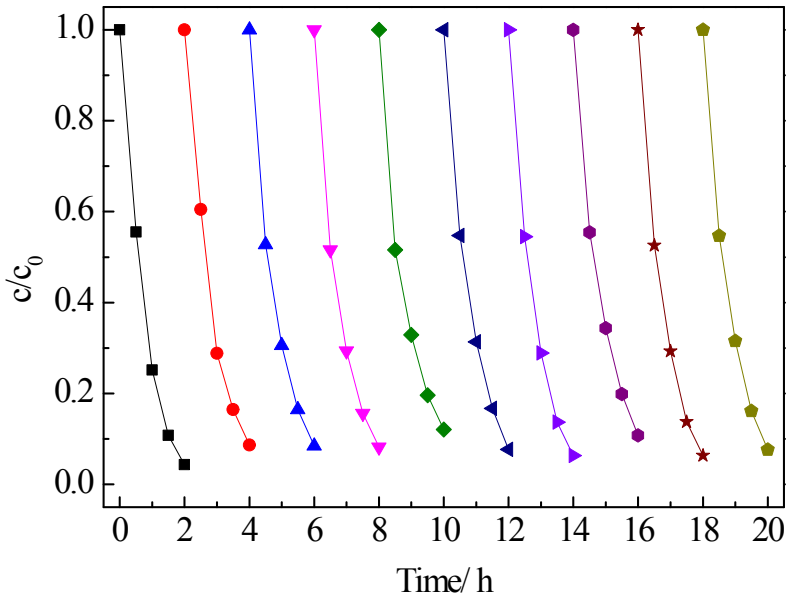

Figure S10. Cycling performance of the W, N co-doped TiO_2 nanobelt thin film for the photodegradation of 0.005 mM rhodamine B aqueous solution, under the Xe-lamp illumination.

References

[1] Y.S. Luo, J.S. Luo, W.W. Zhou, X.Y. Qi, H. Zhang, D.Y.W. Yu, C.M. Li, H.J. Fan, T. Yu, *J. Mater. Chem. A*, 2013, **1**, 273.

[2] B.T. Liu, L.L. Peng, *J. Alloys Compd.*, 2013, **571**, 145.

[3] W.J. Zhou, H. Liu, J.Y. Wang, D. Liu, G.J. Du, J.J. Cui, *ACS Appl. Mater. Interfaces*, 2010, **2**, 2385.